Bax transmembrane domain interacts with prosurvival Bcl-2 proteins in biological membranes

Vicente Andreu-Fernández[a,b,c], Mónica Sancho[a], Ainhoa Genovés[a], Estefanía Lucendo[a], Franziska Todt[b], Joachim Lauterwasser[b,d], Kathrin Funk[b,d], Günther Jahreis[e], Enrique Pérez-Payá[a,f,1], Ismael Mingarro[c,2], Frank Edlich[b,g,2], and Mar Orzáez[a,2]

[a]Laboratory of Peptide and Protein Chemistry, Centro de Investigación Príncipe Felipe, E-46012 Valencia, Spain; [b]Institute for Biochemistry and Molecular Biology, University of Freiburg, 79104 Freiburg, Germany; [c]Departament de Bioquímica i Biologia Molecular, Estructura de Recerca Interdisciplinar en Biotecnología i Biomedicina, Universitat de València, 46100 Burjassot, Spain; [d]Faculty of Biology, University of Freiburg, 79104 Freiburg, Germany; [e]Department of Biochemistry/Biotechnology, Martin Luther University Halle-Wittenberg, 06120 Halle, Germany; [f]Instituto de Biomedicina de Valencia, Instituto de Biomedicina de Valencia–Consejo Superior de Investigaciones Científicas, 46010 Valencia, Spain; and [g]BIOSS, Centre for Biological Signaling Studies, University of Freiburg, 79104 Freiburg, Germany

Edited by William F. DeGrado, School of Pharmacy, University of California, San Francisco, CA, and approved November 29, 2016 (received for review July 28, 2016)

The Bcl-2 (B-cell lymphoma 2) protein Bax (Bcl-2 associated X, apoptosis regulator) can commit cells to apoptosis via outer mitochondrial membrane permeabilization. Bax activity is controlled in healthy cells by prosurvival Bcl-2 proteins. C-terminal Bax transmembrane domain interactions were implicated recently in Bax pore formation. Here, we show that the isolated transmembrane domains of Bax, Bcl-x_L (B-cell lymphoma-extra large), and Bcl-2 can mediate interactions between Bax and prosurvival proteins inside the membrane in the absence of apoptotic stimuli. Bcl-2 protein transmembrane domains specifically homooligomerize and heterooligomerize in bacterial and mitochondrial membranes. Their interactions participate in the regulation of Bcl-2 proteins, thus modulating apoptotic activity. Our results suggest that interactions between the transmembrane domains of Bax and antiapoptotic Bcl-2 proteins represent a previously unappreciated level of apoptosis regulation.

apoptosis | Bcl-2 | mitochondria | oligomerization | transmembrane

The mitochondrial apoptosis program can activate the proapoptotic Bcl-2 (B-cell lymphoma 2) protein Bax (Bcl-2 associated X, apoptosis regulator) in response to stress, resulting in outer mitochondrial membrane (OMM) permeabilization and the release of cytochrome *c* (cyt *c*) and other proteins of the intermembrane space into the cytosol. The Bcl-2 family controls Bax activity and thus the integrity of the OMM (1–3). Prosurvival Bcl-2 proteins harbor four Bcl-2 homology domains [BH1–4, as represented by Bcl-2, Bcl-x_L (B-cell lymphoma-extra large), or Mcl-1] and counteract proapoptotic Bcl-2 proteins with three BH domains (BH1–3; e.g., Bax or Bak). The diverse group of BH3-only proteins regulates both prosurvival and proapoptotic Bcl-2 proteins. Prosurvival Bcl-2 proteins either inhibit Bax via direct interaction or by sequestering "activator" BH3-only proteins, thus preventing their interaction with Bax (4–9).

In healthy cells, newly synthesized Bax initially translocates to the OMM, but efficiently retrotranslocates to the cytoplasm, depending on prosurvival Bcl-2 proteins (10, 11). Bax shuttling thus establishes an equilibrium between cytosolic and mitochondrially anchored molecules (10, 12), determining the cellular response to apoptotic stress (13). Upon the induction of apoptosis, Bax and Bak interact and at least partially insert into the OMM (14–16). Regulatory interactions between Bax and other Bcl-2 proteins can only be observed in the presence of the OMM or liposomes (17, 18). Recent studies suggest that Bax is inserted in mitochondrial membranes as a monomer that oligomerizes once inserted (19–21). These studies also have shown that Bcl-x_L inhibits Bax by dissociating Bax oligomers. However, the contribution of the different protein domains to oligomer formation and apoptosis modulation within the membrane is still unclear.

Transmembrane domains (TMDs) can mediate protein–protein interactions within membranes and be involved in signal transduction across bilayers via changes in the oligomeric state or protein conformation (22–24). The Bax TMD targets fusion proteins to the OMM; its deletion results in cytosolic Bax localization and impaired Bax activity (25). Analysis of the active Bax membrane topology suggests that the TMD could play a central role in Bax oligomerization (26). Förster resonance energy transfer studies have shown that Bax forms homooligomers in the mitochondria through TMD interactions (27). Bcl-x_L–mediated Bax retrotranslocation into the cytosol depends on the Bcl-x_L TMD, suggesting the involvement of TMD interactions in Bax inhibition (13). In addition, distance mapping of cysteine-labeled Bax variants in large unilamellar vesicles suggests a role of the Bax TMD in the formation of potential Bax pore structures (28). Thus, TMD interactions could be involved in Bax regulation, oligomerization, and pore formation.

Here, we report the self-association and interaction of the TMDs of Bax, Bcl-2, and Bcl-x_L in the biological membranes of living cells in the absence and presence of apoptosis induction. The TMDs mediate homooligomerization and heterooligomerization between proapoptotic Bax, and prosurvival Bcl-2 and Bcl-x_L members independent of extramembrane protein regions, modulating the response to apoptosis signaling.

Significance

Bcl-2 (B-cell lymphoma 2) proteins are key regulators of apoptosis. The recruitment of the predominantly cytosolic Bcl-2 protein Bax (Bcl-2 associated X, apoptosis regulator) to the mitochondria is associated with mitochondrial outer membrane permeabilization and apoptosis. We report specific interactions between the transmembrane domains (TMDs) of Bax and the prosurvival Bcl-x_L (B-cell lymphoma-extra large) and Bcl-2 proteins. Our results demonstrate that these interactions occur in nonapoptotic human cells and participate in the regulation of Bcl-2 proteins, introducing the concept of modulation mitochondrial apoptosis signaling by TMD-mediated Bcl-2 protein interactions.

Author contributions: V.A.-F., M.S., A.G., E.P.-P., I.M., F.E., and M.O. designed research; V.A.-F., M.S., A.G., E.L., F.T., J.L., G.J., and M.O. performed research; K.F. and M.O. contributed new reagents/analytic tools; I.M., F.E., and M.O. analyzed data; and I.M., F.E., and M.O. wrote the paper.

The authors declare no conflict of interest.

This article is a PNAS Direct Submission.

Freely available online through the PNAS open access option.

[1]Deceased May 28, 2013.

[2]To whom correspondence may be addressed. Email: morzaez@cipf.es, Ismael.Mingarro@uv.es, or frank.edlich@biochemie.uni-freiburg.de.

This article contains supporting information online at www.pnas.org/lookup/suppl/doi:10.1073/pnas.1612322114/-/DCSupplemental.

Results and Discussion

Bax, Bcl-x_L, and Bcl-2 TMDs Homooligomerize in *E. coli* Membranes. Interactions between Bcl-2 proteins require membranes (29, 30). Therefore, the potential homooligomerization of Bax, Bcl-2, and Bcl-x_L TMDs was analyzed in living cells by using the ToxRed system (31). In this assay, TMDs were inserted between the transcriptional activation domain (ToxR) and maltose-binding protein (MBP), targeted to the periplasm (32). Transcriptional activation of the cholera toxin promoter strictly depends on ToxR oligomerization (33). Consequently, TMD oligomerization resulted in red fluorescent protein (RFP) expression (Fig. 1*A*). The level of fluorescence is proportional to the analyzed oligomerization. Fusion protein functionality, orientation, and membrane insertion were controlled by the growth of mutant *Escherichia coli* on maltose as the sole carbon source dependent on MBP activity in the periplasm (Fig. S1). The TMDs of Bcl-x_L and Bcl-2 induced as much RFP fluorescence and therefore oligomerization as the positive control, glycophorin A (GpA) TMD (Fig. 1*B*). Similar levels of Bax TMD generated the highest fluorescence levels (Fig. 1*B*). The emission spectra of ToxRed chimeras corroborate the formation of Bcl-2 protein homooligomers (Fig. S2). Interestingly, the amino acid sequences of the Bax, Bcl-x_L, and Bcl-2 TMDs (Table 1) revealed central glycine residues as potential sites for strong helix–helix interactions through ridge-into-grove arrangements, as observed for other interacting TMDs (24, 34–37). These glycine residues are evolutionarily conserved (Fig. S3). Structural studies have demonstrated that conserved glycine residues rarely face lipids, and many of them participate in close helix–helix packing (38). Accordingly, Fig. 1*C* shows disruptive effects for mutations Bcl-2 G227I, Bcl-x_L G222I, and, to a lesser extent, for Bax G179I (similar to the GpA G83I mutant) (39). The helix-breaking G179P mutation [similar to GpA (40)] resulted in an even-more-prominent disruption of Bax TMD homooligomerization, whereas mutation of the conserved Bax F176 had no effect. In all cases, expression levels, as determined by Western blotting, were comparable (Fig. 1 *B* and *C*). Furthermore, appropriate membrane insertion of chimeric proteins was confirmed (Fig. S4). Therefore, the TMDs of Bax, Bcl-2, and Bcl-x_L mediate specific and efficient homooligomerization in a biological membrane.

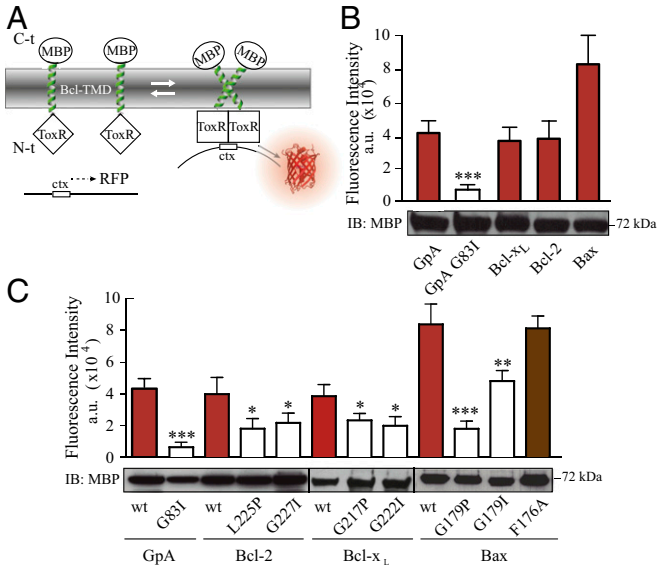

Fig. 1. Bax, Bcl-x_L, and Bcl-2 TMDs homooligomerize in membranes. (*A*) TMD constructs fused to ToxR were expressed in the inner membrane of *E. coli*. The TMD interaction reconstituted active ToxR and activated *ctx* promoter-regulated RFP expression. The C-terminal MBP domain was exposed to the periplasm. (*B*) ToxR-TMD-MBP constructs (Table 1) were transformed into MM39 cells. The fluorescence signal (λ_{exc} 570, λ_{em} 620 nm) obtained with the ToxRed system for Bax, Bcl-x_L, and Bcl-2 TMDs is shown. Red bars highlight interactions. The GpA TMD and nondimerizing TMD GpA G83I variant served as positive and negative controls, respectively. Western blotting of MBP revealed equivalent expression levels. (*C*) Homooligomerization assay of wild-type and variants of the Bax, Bcl-x_L, and Bcl-2 TMDs. Fusion protein functionality, orientation, and membrane insertion of all variants were controlled by growth on minimum medium (Fig. S4). Reduction in fluorescence indicates the disruption of homooligomerization (white bars). Results obtained with mutations that apparently do not interfere with homooligomerization are depicted in brown. Error bars represent the mean ± SD; $n \geq 3$. Western blotting of MBP revealed equivalent expression levels for all chimeras. *P* values according to Dunnett's test are displayed. *$P < 0.05$; **$P < 0.01$; ***$P < 0.001$.

Table 1. Sequences of the TMDs of human Bax, Bcl-x_L, and Bcl-2 proteins

Protein	Accession no.	Amino acid sequence
Bcl-x_L	NP_612815	^{210}FNRWFLT**G**MTVA**G**VVLLGSLFSR^{232}
Bcl-2	NP_000624	^{214}WLSLKTLLSLALV**G**ACITLGAYL^{236}
Bax	Q07812	^{169}TWQTVTI*F*VA**G**VLTASLTIW^{188}

Central glycine residues are shown in bold, and mutated Phe^{176} from Bax is in italics.

Bax, Bcl-x_L, and Bcl-2 TMDs Form Oligomers in Mitochondrial Membranes. Next, we analyzed the self-association capacity of Bax, Bcl-x_L, and Bcl-2 TMDs in nonapoptotic human cells using bimolecular fluorescence complementation (BiFC) assays (41). TMDs were fused with two nonfluorescent fragments (VN: 1–155 amino acids, I152L; and VC: 155–238 amino acids, A206K) of the venus fluorescent protein to assess whether TMD interactions would reconstitute fluorescence of venus (Fig. 2*A*) (42). VN and VC constructs fused to the same TMD were cotransfected in HCT116 colon carcinoma cells. This process, indeed, resulted in Bax, Bcl-2, and Bcl-x_L TMD homooligomerization in the absence of apoptotic stimuli (Fig. 2*B*). The nonoligomerizing TMD of the abundant mitochondrial Tom20 protein was used as a negative control for overcrowding. Bcl-x_L oligomerization is still controversial; some cross-linking experiments suggest oligomer formation, whereas other studies using detergents or structural data in nanodiscs have revealed monomers (43). However, extraction of transmembrane proteins with detergents could dissociate them, and nanodisc studies are highly dependent on the lipid composition (44). A striking advantage of the BiFC assays is the observation of interactions in eukaryotic membranes. The Western blot analysis confirmed comparable expression levels of the VN and VC constructs. Therefore, the observed fluorescence values indicate different association levels and agree with the results obtained in the ToxRed system (Fig. 1*B* and Fig. S5), where self-association of the proapoptotic Bax TMD caused the highest fluorescence signal. The analysis of the intracellular distribution of TMD fusion proteins by confocal microscopy revealed mitochondrial localization (Fig. 2*C*).

Next, single amino-acid substitutions were introduced into the TMDs to analyze the sequence specificity of TMD homooligomerization (Fig. 2*D*). The subcellular distribution of chimeric constructs was also corroborated by cellular fractionation (Fig. 2*E*). In agreement with ToxRed homooligomerization experiments, strong interference by Bax G179P (see also Fig. 2*C*, bottom row), Bcl-2 G227I, and Bcl-x_L G222I was observed, whereas Bax F176A again exhibited no difference from the wild-type construct. The Bcl-2 L225P and Bcl-x_L G217P mutants also exhibited strong interference with TMD oligomerization. Therefore, Bax, Bcl-2, and Bcl-x_L TMDs form specific homooligomers within the OMM.

Bax TMD Interacts with Prosurvival Bcl-2 Protein TMDs. Because of the specific homooligomerization of the Bax, Bcl-2, and Bcl-x_L TMDs in nonapoptotic cells, the possibility of heterooligomerization and regulatory interactions between these TMDs was tested.

BIOCHEMISTRY

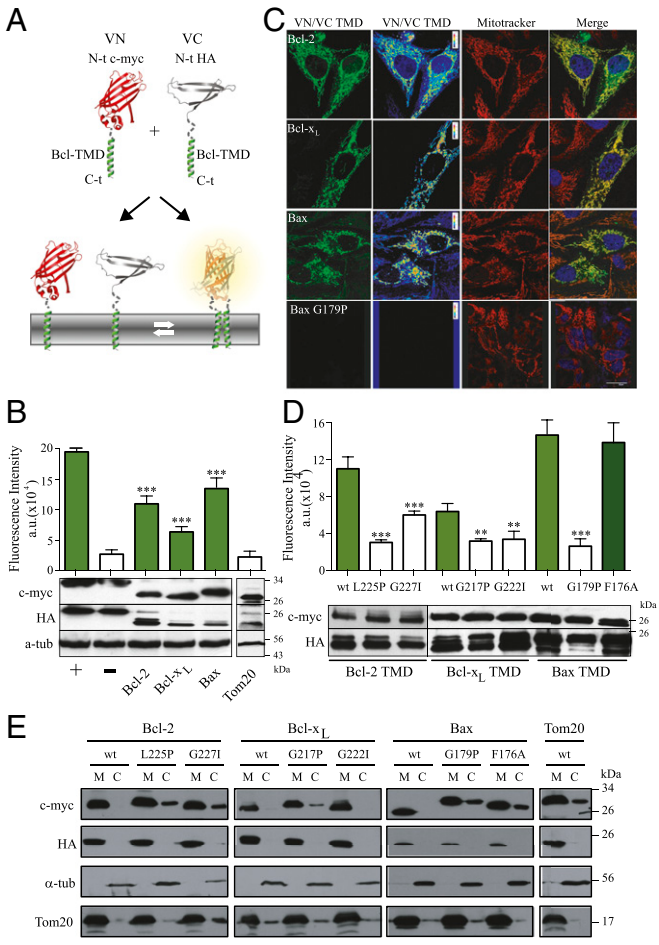

Fig. 2. Bax, Bcl-2, and Bcl-x_L homooligomerize in the OMM. (*A*) BiFC assay analyzing TMD homooligomerization by reconstitution of venus fluorescence from separate N and C termini fragments fused to TMD segments. (*B*) Bax, Bcl-2, and Bcl-x_L TMD homooligomerization measured by BiFC in HCT116 cells. Fusions of b-Fos and b-Jun protein domains were used as positive controls (+), and the Δb-Fos/bJun pair served as a negative control (–); $n = 3$. Significant increases compared with negative control were analyzed by using Dunnett's multiple comparison test (95% confidence interval). Chimeric protein expression of VN (c-myc) and VC (HA) constructs is compared in *B*, *Lower*; α-tubulin was used as loading control. (*C*) Confocal images of HCT116 cells transfected with VC and VN constructs of the Bcl-2 and Bcl-x_L Bax, and Bax G197P TMDs. Formation of homooligomers (green and rainbow scale, first and second column, respectively) and mitochondria (red, third column), colocalized (yellow, fourth column). (Scale bar, 20 μm.) (*D*) Self-association assays of wild-type and single amino acid substitution variants of the Bax, Bcl-2, and Bcl-x_L TMDs measured by BiFC in HCT116 cells. Error bars represent the mean ± SD, $n \geq 3$. *P* values according to Dunnett's test are displayed. **P* < 0.05; ***P* < 0.01; ****P* < 0.001. (*E*) Subcellular fractionation of HCT116 cells transfected with TMD constructs was controlled by using Tom20 (mitochondrial fraction; M) and α-tubulin (cytosol; C).

To this end, we analyzed the competition between homomerization of ToxR fusion proteins and their heterooligomerization with fusion proteins with the disabled ToxR DNA binding domain (ToxR*; Fig. 3*A*). Disabled ToxR* fusion proteins can interact with ToxR proteins in a dominant-negative fashion; the resulting decrease in RFP expression thus indicates the ratio between homooligomerization and heterooligomerization. In this assay, competition between homooligomer and heterooligomer formation with similar affinities results in a 50% decrease in fluorescence (31).

The Bax TMD has a strong tendency to self-associate (Figs. 1*B* and 3*B*). As expected, this signal was attenuated by coexpressing ToxR*/BaxTMD, whereas the ToxR*/GpATMD did not interfere with RFP expression (Fig. 3*B*). Interestingly, both TMDs derived from prosurvival Bcl-2 or Bcl-x_L proteins interfered with Bax TMD homooligomerization to at least the extent of the Bax TMD. These results suggest a strong capability of the TMDs of prosurvival Bcl-2 proteins to heterooligomerize with the Bax TMD. Accordingly, the Bax TMD reduced Bcl-x_L and Bcl-2 homooligomerization (Fig. 3 *C* and *D*). Strikingly, the Bcl-2 and Bcl-x_L TMDs did not interfere with each other's homooligomerization, suggesting an absence of heterooligomerization between both prosurvival Bcl-2 TMDs (Fig. 3 *C* and *D*). These results suggest that the interactions of prosurvival Bcl-2 protein TMDs enable heterooligomerization with Bax. Interactions between the Bax TMD and TMDs of prosurvival Bcl-2 proteins could participate in Bax regulation, because the membrane-bound form of Bcl-x_L has been described to insert only its TMD into the membrane (43). Therefore, the influence of TMD interactions on Bax regulation was tested by analyzing isolated mitochondria permeabilization in HCT116 Bak knockout (KO) cells in the presence or absence of corresponding Bax, Bcl-x_L, Bcl-2, and Fis1 TMD segments. The presence of high Bcl-x_L or Bcl-2 TMD concentrations inhibited the release of Smac from mitochondria (Fig. 3*E*). These results show that heterooligomerization between Bax TMD and prosurvival Bcl-2 protein

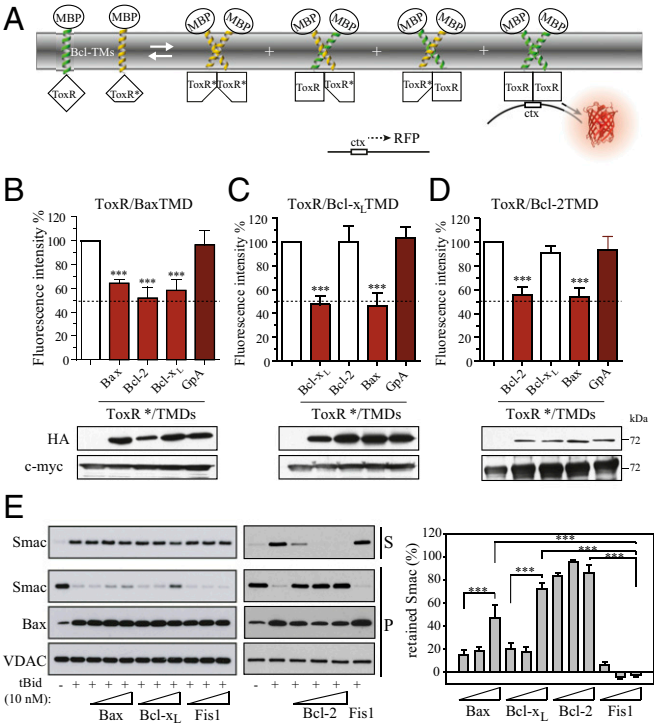

Fig. 3. The Bax TMD interacts with antiapoptotic Bcl-x_L and Bcl-2 TMDs. (*A*) Dominant-negative ToxR assay to analyze Bcl-2 protein TMD heterooligomerization. Coexpression of TMD constructs fused to wild-type ToxR (green) and TMD constructs fused to an inactive ToxR* mutant (yellow) in *E. coli* can result in heterooligomerization, leading to reduced RFP synthesis. (*B*) Effect of the Bax, Bcl-2, and Bcl-x_L TMDs on ToxR/Bax TMD homooligomerization. The GpA TMD served as a control. (*C*) Effect of the Bax, Bcl-2, and Bcl-x_L TMDs on Bcl-x_L TMD homooligomerization as in *B*. (*D*) Effect of the Bax, Bcl-2, and Bcl-x_L TMDs on Bcl-2 TMD homooligomerization as in *B*. The GpA TMD served as a control. (*E*) Smac release by endogenous Bax with and without tBid in the absence and presence of the Bax, Bcl-x_L, Bcl-2, or Fis1 TMD peptides from purified HCT116 Bak KO mitochondria. Smac was monitored in the supernatant (S) and pellet (P) by Western blot. Bax and VDAC served as controls. Error bars represent the mean ± SD, $n \geq 3$. *P* values according to Dunnett's test are displayed. **P* < 0.05; ***P* < 0.01; ****P* < 0.001.

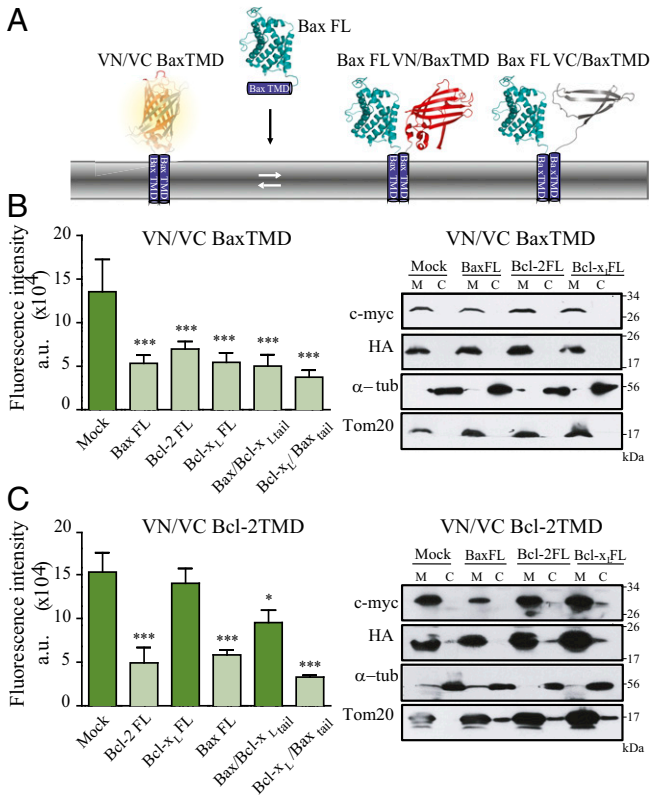

Fig. 4. Bcl-2 protein TMDs interact with full-length Bcl-2 proteins. (*A*) Heterooligomerization studies with the BiFC system using venus fluorescent protein (VFP) reconstituted from VN/VC BaxTMD chimeras and full-length Bax (BaxFL). In this assay, a decrease in fluorescence indicates the formation of heterooligomers between venus-derived chimeras and full-length Bcl-2 proteins. (*B*) Oligomerization analysis of the Bax TMD in the presence of full-length Bax, Bcl-2, Bcl-x_L, Bax-Bcl-$x_{L\ tail}$, and Bcl-x_L-Bax_{tail}. VFP reconstitution by VN/VC BaxTMD chimeras was challenged with the indicated full-length proteins in HCT116 cells (*B*, *Left*). Subcellular fractionation showed mitochondrial (M) localization of VN/Bax and VC/Bax in the absence or presence of full-length proteins. C indicates the cytosolic fraction. (*C*) Analysis of Bcl-2 TMD oligomerization in the presence of full-length Bax, Bcl-2, Bcl-x_L, Bax–Bcl-$x_{L\ tail}$, and Bcl-x_L–Bax_{tail} proteins in HCT116 cells. Subcellular fractionation showed Bcl-2 TMD-derived constructs localization in the absence or the presence of full-length proteins. Tom20 and α-tubulin served as controls. $*P < 0.05$; $***P < 0.001$.

TMDs interferes with Bax-induced OMM permeabilization. However, other mechanisms, such as competition for a common binding site or interference in the interaction with other OMM components, could also account for the observed effects. Bcl-x_L TMD-dependent inhibition of OMM permeabilization is not complete, because cyt *c* is still released (Fig. S6). Lack of inhibition by the Bax TMD is particularly interesting, because the peptide concentration exceeded the native Bax protein concentrations. Therefore, symmetric Bax, and perhaps Bak oligomers, as recently suggested (27, 45), could tolerate the association of multiple TMDs. Alternatively, other oligomeric Bax structures could be more prominent in OMM permeabilization.

Bax TMD Interacts with Full-Length Proteins. Next, we tested the potential of Bax, Bcl-2, and Bcl-x_L TMDs to interact with full-length proteins. Self-associating VN/VC-BaxTMD or VN/VC-Bcl-2TMD chimeras that reconstitute the venus fluorescent protein were coexpressed with antiapoptotic and proapoptotic full-length proteins in HCT116 cells (Fig. 4*A*). BaxTMD homooligomerization was disturbed in the presence of full-length Bax, Bcl-2, and Bcl-x_L (Fig. 4*B* and Fig. S7*A*). Therefore, full-length proteins bind to the Bax TMD-derived chimeras, corroborating the interactions between the isolated TMD segments (Fig. 3 *B–D*). Interestingly, Bax and Bcl-2 proteins interfered with Bcl-2 TMD homooligomerization, but Bcl-x_L protein did not (Fig. 4*C* and Fig. S7*B*). The mitochondrial location of overexpressed TMD constructs was corroborated by subcellular fractionation experiments (Fig. 4 *B* and *C*, *Right*). The specificity and TMD dependence of these interactions were tested by replacing the Bax TMD with the corresponding Bcl-x_L TMD segment in the full-length Bax protein (Bax/Bcl-x_{Ltail}). Bax/Bcl-x_{Ltail} interfered with Bax, but slightly altered Bcl-2 TMD homooligomerization (Fig. 4 *B* and *C*). On the other hand, the reciprocal chimera harboring the BaxTMD in full-length Bcl-x_L (Bcl-x_L/Bax_{tail}) bound to Bax and Bcl-2 (Fig. 4 *B* and *C*). Then, the interaction between the TMDs of Bax and Bcl-2 and full-length proteins is specific and depends on the TMD of the Bcl-2 protein. These results were also corroborated in Bax/Bak double-KO (DKO) cells (Figs. S8 and S9).

Bax TMD Modulates Interactions with Endogenous Proteins and Activates Apoptosis. The Bcl-x_L TMD is involved in Bax retrotranslocation, and we thus focused our studies on the interactions between both TMDs (13). A fusion of the Bax TMD to the C terminus of the biotin ligase BirA (BirA/BaxTMD) biotinylated endogenous Bax and Bcl-x_L in nonapoptotic HCT116 cells (Fig. 5 *A* and *B*). These results imply binding between Bax TMD and endogenous Bax and Bcl-x_L proteins in the absence of apoptotic stimuli and independent of cytosolic (extramembranous) domain

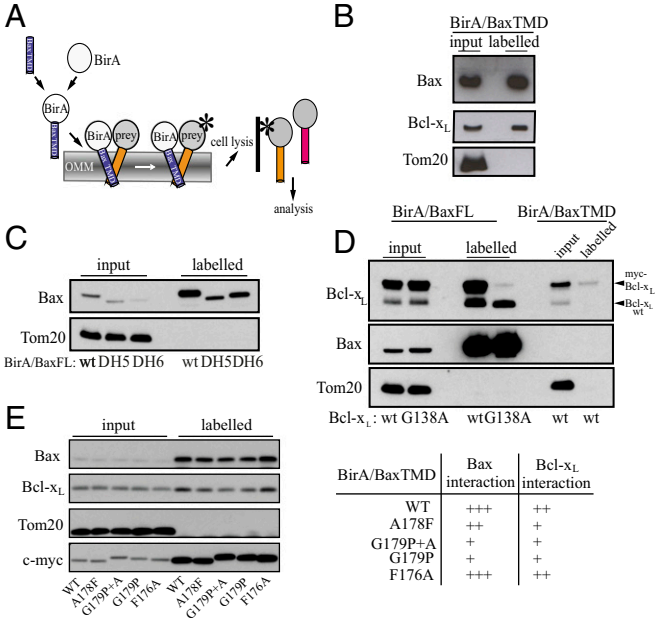

Fig. 5. Bax TMD interacts with endogenous Bax and Bcl-x_L. (*A*) The BirA in situ proximal biotinylation assay was used to identify interactions between the Bax TMD and endogenous Bax and Bcl-x_L proteins in human cells. After the expression of BirA/BaxTMD, proteins interacting with Bax TMD (blue) were labeled with biotin (star) by BirA. Crude cell extract was subsequently applied to a biotin affinity matrix (solid line). Bound (labeled) proteins were analyzed by SDS/PAGE and Western blot. (*B*) Input and labeled proteins of the biotin affinity matrix from HCT116 cells expressing BirA/BaxTMD fusion were analyzed by Western blot. Tom20 served as a control. (*C*) BirA fusion assay analyzing BirA/BaxFL-interactions with wild-type Bax compared with Bax ΔH5 and Bax ΔH6 present in the labeled fraction (L) compared with the input (I) by Western blot. $n = 3$. (*D*) BirA fusion assay comparing BirA/BaxFL and BirA/ BaxTMD interactions with either endogenous Bcl-x_L (Bcl-x_L WT) or ectopically expressed wild-type myc-Bcl-x_L or the myc-Bcl-x_L G138A variant by Western blot. Tom20 serves as control. $n = 3$. (*E*) The BirA fusion assay was used to identify interactions between Bax TMD mutants and endogenous Bax and Bcl-x_L proteins in human cells.

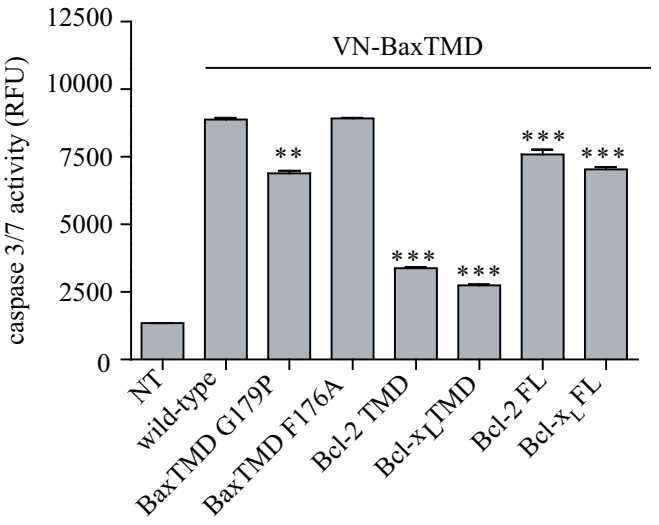

Fig. 6. TMD interactions modulate apoptotic response. Effect of VN/BaxTMD variants, VN/Bcl-2TMD and VN/Bcl-x_LTMD chimeric proteins, or Bcl-2 and Bcl-x_L full-length proteins on caspase-3/7 activity induced by VN-BaxTMD in HCT116 cells is shown. Caspase 3/7 activity was analyzed in cytosolic extracts 24 h after transfection. Error bars represent the mean ± SD, $n = 3$. P values according to Dunnett's test are displayed. $^{**}P < 0.01$; $^{***}P < 0.001$.

interactions. Our results are supported by Bak (and Bax) TMD interfaces mediating homooligomerization in the absence of BH3-dependent interactions (45). Mutant Bax proteins lacking either alpha 5 (Δ5) or alpha 6 (Δ6) helices, which are potentially relevant for membrane insertion and pore formation (19, 26, 28, 46), retained the capacity for Bax association in mitochondrial membranes (Fig. 5*C*), emphasizing the role of the TMDs in early protein interactions. Both BirA/BaxFL and BirA/BaxTMD bound to wild-type Bcl-x_L (Fig. 5*D*). This binding was strongly reduced when cells were cotransfected with the nonfunctional Bcl-x_L G138A mutant (47). Strikingly, some capacity for heterooligomer formation was retained (Fig. 5*D*) and matches the Bax TMD capability of oligomer formation, corroborating the contribution of Bax TMD interactions with prosurvival Bcl-x_L. Mutations in the BirA/BaxTMD construct that decrease Bax homooligomerization, such as G179P, provoked a similar decrease in Bcl-x_L biotinylation (Fig. 5*E*), suggesting at least a partial common interface for heterooligomerization and homooligomerization.

Together, our results demonstrate that interactions between the TMDs of Bax and Bcl-x_L occur in the OMM of human cells before the induction of apoptosis. The analysis of a potential role of TMD interactions in apoptosis induction revealed that the ectopic expression of the BaxTMD in HCT116 cells induces caspase-3/7 activation (Fig. 6). BaxTMD G179P, but not BaxTMD F176A, interferes with this activation, in good agreement with the impact of these mutants on oligomerization in Fig. 2*D*. Furthermore, cotransfection with antiapoptotic Bcl-2- and Bcl-x_L TMD-derived constructs or with full-length proteins significantly reduced apoptosis activation (Fig. 6). Therefore, Bcl-2 protein TMD interactions are involved in mitochondrial apoptosis signaling.

Conclusion

Antiapoptotic and proapoptotic Bcl-2 proteins regulate mitochondrial apoptosis signaling, and thus the cell fate, by dynamic interactions. Interplay between the BH3 domains and hydrophobic grooves of the respective interaction partner have been characterized (48). In the present study, we discovered interactions between the TMDs of Bax, Bcl-2, and Bcl-x_L that occur in nonapoptotic cells and modulate mitochondrial apoptosis signaling. The consistent picture that emerges from these studies is that Bcl-2 and Bcl-xL TMDs could have the ability to regulate Bax pore-forming activity by means of direct competition, leading to the formation of heterooligomers that abate Bax homooligomer formation and OMM permeabilization. The existence of Bax TMD interactions has been proposed based on cross-linking experiments (49, 50) and 3D models (28) and has been suggested to contribute to the enlargement of the Bax pore (51). Although not as tight as hydrophobic groove and BH3 domain interactions, TMD-TMD interactions are sufficient for heterooligomerization and homooligomerization of Bcl-2 proteins. Therefore, Bax dimers and oligomers could facilitate lateral sorting in the OMM or the formation of Bcl-2 protein-containing complexes (52). TMD–TMD interactions are consistent with models of Bax activation, suggesting separation of helices α5 and α6 (27, 53) and the concerted insertion of both helices into the OMM (51, 54). Conversely, Bax activation according to the clamp model would require a sequential mechanism to allow formation of antiparallel TMD interactions (28). The observation of TMD–TMD interactions between Bcl-2 proteins in proliferating cells further emphasizes the necessity to assess the protein conformation of Bax and other Bcl-2 proteins. These new surfaces of protein–protein interaction among proapoptotic and prosurvival members could represent attractive targets for selective drug design.

Methods

Methods are fully described in *SI Methods*. ToxRed chimeric constructs were generated by specific primer annealing of Bcl-2 protein TMDs in the HindIII/XhoI restriction sites of ToxRed vectors (Table 1 and Table S1). The maltose complementation assay was performed as described (39, 55).

ToxRed Oligomerization Assays. ToxR–Bcl-2 TMD constructs (Table S1) were transformed into the *malE* mutant *E. coli* MM39 strain. For RFP measurements, 24-well plates were adjusted to equivalent growth (OD_{600} 0.6–0.8), and the RFP emission spectra were collected by a Wallac 1420 Workstation (λ_{exc} 560 and λ_{em} 595 nm).

BiFC-TMD Assays. BiFC assays were performed as described (56). An improved BiFC assay with a high signal-to-noise ratio was selected to avoid background interference (57, 58). The system was adapted to clone Bax, Bcl-x_L, and Bcl-2 TMDs at the C terminus of venus protein fragments, according to their natural topology in full-length proteins.

BirA Interaction Partner Identification. HCT116 Bax/Bak DKO cells were transfected with pcDNA3-mycBioID-Bax plasmid, resulting in the expression of myc-tagged BirA/Bax fusion. The cell lysate was incubated with streptavidin agarose beads (Thermo) at 4 °C overnight. Input and bead samples were resolved on a 10% (wt/vol) SDS/PAGE and analyzed by Western blot for the indicated proteins.

ACKNOWLEDGMENTS. We thank Prof. W. DeGrado (University of California, San Francisco School of Pharmacy) for kindly providing the ToxR plasmids; Profs. R. Youle and B. Vogelstein for kindly providing the human colorectal carcinoma HCT116 cells; Prof. D. Langosch for critical reading of the manuscript and helpful suggestions; and Maria J. Garcia-Murria, Sylvia Liebscher, and Alicia García-Jareño for technical assistance. This work was supported by Spanish Ministry of Economy and Competitiveness Grants BFU2016-79487, SAF2014-52614-R, and BEFPI/2013/A/046; Generalitat Valenciana Grant PROMETEOII/2014/061; the Emmy Noether program; the Heisenberg program and the Sonderforschungsbereich 746 of the German Research Council (Deutsche Forschungsgemeinschaft); and the Centre for Biological Signalling Studies (BIOSS, EXC-294) funded by the Excellence Initiative of the German Federal and State Governments. V.A.-F. and E.L. were supported by Generalitat Valenciana Grants BEFPI/2013/A/046 and ACIF/2016/019.

1. Chipuk JE, Green DR (2008) How do BCL-2 proteins induce mitochondrial outer membrane permeabilization? *Trends Cell Biol* 18(4):157–164.
2. Youle RJ, Strasser A (2008) The BCL-2 protein family: Opposing activities that mediate cell death. *Nat Rev Mol Cell Biol* 9(1):47–59.
3. Billen LP, Kokoski CL, Lovell JF, Leber B, Andrews DW (2008) Bcl-XL inhibits membrane permeabilization by competing with Bax. *PLoS Biol* 6(6):e147.
4. Kim H, et al. (2006) Hierarchical regulation of mitochondrion-dependent apoptosis by BCL-2 subfamilies. *Nat Cell Biol* 8(12):1348–1358.

5. Kuwana T, et al. (2005) BH3 domains of BH3-only proteins differentially regulate Bax-mediated mitochondrial membrane permeabilization both directly and indirectly. *Mol Cell* 17(4):525–535.
6. Letai A, et al. (2002) Distinct BH3 domains either sensitize or activate mitochondrial apoptosis, serving as prototype cancer therapeutics. *Cancer Cell* 2(3):183–192.
7. Llambi F, et al. (2011) A unified model of mammalian BCL-2 protein family interactions at the mitochondria. *Mol Cell* 44(4):517–531.
8. Willis SN, et al. (2007) Apoptosis initiated when BH3 ligands engage multiple Bcl-2 homologs, not Bax or Bak. *Science* 315(5813):856–859.
9. Chen L, et al. (2005) Differential targeting of prosurvival Bcl-2 proteins by their BH3-only ligands allows complementary apoptotic function. *Mol Cell* 17(3):393–403.
10. Edlich F, et al. (2011) Bcl-x(L) retrotranslocates Bax from the mitochondria into the cytosol. *Cell* 145(1):104–116.
11. Wolter KG, et al. (1997) Movement of Bax from the cytosol to mitochondria during apoptosis. *J Cell Biol* 139(5):1281–1292.
12. Gavathiotis E, Reyna DE, Davis ML, Bird GH, Walensky LD (2010) BH3-triggered structural reorganization drives the activation of proapoptotic BAX. *Mol Cell* 40(3): 481–492.
13. Todt F, Cakir Z, Reichenbach F, Youle RJ, Edlich F (2013) The C-terminal helix of Bcl-x(L) mediates Bax retrotranslocation from the mitochondria. *Cell Death Differ* 20(2): 333–342.
14. Antonsson B, Montessuit S, Lauper S, Eskes R, Martinou JC (2000) Bax oligomerization is required for channel-forming activity in liposomes and to trigger cytochrome c release from mitochondria. *Biochem J* 345(Pt 2):271–278.
15. Eskes R, et al. (1998) Bax-induced cytochrome C release from mitochondria is independent of the permeability transition pore but highly dependent on Mg2+ ions. *J Cell Biol* 143(1):217–224.
16. Wei MC, et al. (2001) Proapoptotic BAX and BAK: A requisite gateway to mitochondrial dysfunction and death. *Science* 292(5517):727–730.
17. Roucou X, Montessuit S, Antonsson B, Martinou JC (2002) Bax oligomerization in mitochondrial membranes requires tBid (caspase-8-cleaved Bid) and a mitochondrial protein. *Biochem J* 368(Pt 3):915–921.
18. Leber B, Lin J, Andrews DW (2010) Still embedded together binding to membranes regulates Bcl-2 protein interactions. *Oncogene* 29(38):5221–5230.
19. Xu XP, et al. (2013) Three-dimensional structure of Bax-mediated pores in membrane bilayers. *Cell Death Dis* 4:e683.
20. Subburaj Y, et al. (2015) Bax monomers form dimer units in the membrane that further self-assemble into multiple oligomeric species. *Nat Commun* 6:8042.
21. Salvador-Gallego R, et al. (2016) Bax assembly into rings and arcs in apoptotic mitochondria is linked to membrane pores. *EMBO J* 35(4):389–401.
22. Garrity D, Call ME, Feng J, Wucherpfennig KW (2005) The activating NKG2D receptor assembles in the membrane with two signaling dimers into a hexameric structure. *Proc Natl Acad Sci USA* 102(21):7641–7646.
23. Curran AR, Engelman DM (2003) Sequence motifs, polar interactions and conformational changes in helical membrane proteins. *Curr Opin Struct Biol* 13(4):412–417.
24. Sulistijo ES, MacKenzie KR (2006) Sequence dependence of BNIP3 transmembrane domain dimerization implicates side-chain hydrogen bonding and a tandem GxxxG motif in specific helix-helix interactions. *J Mol Biol* 364(5):974–990.
25. Nechushtan A, Smith CL, Hsu YT, Youle RJ (1999) Conformation of the Bax C-terminus regulates subcellular location and cell death. *EMBO J* 18(9):2330–2341.
26. Annis MG, et al. (2005) Bax forms multispanning monomers that oligomerize to permeabilize membranes during apoptosis. *EMBO J* 24(12):2096–2103.
27. Gahl RF, He Y, Yu S, Tjandra N (2014) Conformational rearrangements in the pro-apoptotic protein, Bax, as it inserts into mitochondria: A cellular death switch. *J Biol Chem* 289(47):32871–32882.
28. Bleicken S, et al. (2014) Structural model of active Bax at the membrane. *Mol Cell* 56(4):496–505.
29. Roucou X, Rostovtseva T, Montessuit S, Martinou JC, Antonsson B (2002) Bid induces cytochrome c-impermeable Bax channels in liposomes. *Biochem J* 363(Pt 3):547–552.
30. Lovell JF, et al. (2008) Membrane binding by tBid initiates an ordered series of events culminating in membrane permeabilization by Bax. *Cell* 135(6):1074–1084.
31. Berger BW, et al. (2010) Consensus motif for integrin transmembrane helix association. *Proc Natl Acad Sci USA* 107(2):703–708.
32. Langosch D, Brosig B, Kolmar H, Fritz HJ (1996) Dimerisation of the glycophorin A transmembrane segment in membranes probed with the ToxR transcription activator. *J Mol Biol* 263(4):525–530.
33. Kolmar H, et al. (1995) Membrane insertion of the bacterial signal transduction protein ToxR and requirements of transcription activation studied by modular replacement of different protein substructures. *EMBO J* 14(16):3895–3904.
34. Russ WP, Engelman DM (2000) The GxxxG motif: A framework for transmembrane helix-helix association. *J Mol Biol* 296(3):911–919.
35. Vilar M, et al. (2009) Activation of the p75 neurotrophin receptor through conformational rearrangement of disulphide-linked receptor dimers. *Neuron* 62(1):72–83.
36. MacKenzie KR, Prestegard JH, Engelman DM (1997) A transmembrane helix dimer: structure and implications. *Science* 276(5309):131–133.
37. Orzáez M, Lukovic D, Abad C, Pérez-Payá E, Mingarro I (2005) Influence of hydrophobic matching on association of model transmembrane fragments containing a minimised glycophorin A dimerisation motif. *FEBS Lett* 579(7):1633–1638.
38. Dong H, Sharma M, Zhou HX, Cross TA (2012) Glycines: Role in α-helical membrane protein structures and a potential indicator of native conformation. *Biochemistry* 51(24):4779–4789.
39. Russ WP, Engelman DM (1999) TOXCAT: A measure of transmembrane helix association in a biological membrane. *Proc Natl Acad Sci USA* 96(3):863–868.
40. Orzáez M, Salgado J, Giménez-Giner A, Pérez-Payá E, Mingarro I (2004) Influence of proline residues in transmembrane helix packing. *J Mol Biol* 335(2):631–640.
41. Kerppola TK (2008) Bimolecular fluorescence complementation (BiFC) analysis as a probe of protein interactions in living cells. *Annu Rev Biophys* 37:465–487.
42. Peiró A, et al. (2014) The Tobacco mosaic virus movement protein associates with but does not integrate into biological membranes. *J Virol* 88(5):3016–3026.
43. Yao Y, et al. (2015) Conformation of BCL-XL upon membrane integration. *J Mol Biol* 427(13):2262–2270.
44. Ye X, McLean MA, Sligar SG (2016) Conformational equilibrium of talin is regulated by anionic lipids. *Biochim Biophys Acta* 1858(8):1833–1840.
45. Iyer S, et al. (2015) Bak apoptotic pores involve a flexible C-terminal region and juxtaposition of the C-terminal transmembrane domains. *Cell Death Differ* 22(10): 1655–75.
46. García-Sáez AJ, et al. (2006) Peptides corresponding to helices 5 and 6 of Bax can independently form large lipid pores. *FEBS J* 273(5):971–981.
47. Sedlak TW, et al. (1995) Multiple Bcl-2 family members demonstrate selective dimerizations with Bax. *Proc Natl Acad Sci USA* 92(17):7834–7838.
48. Qian S, Wang W, Yang L, Huang HW (2008) Structure of transmembrane pore induced by Bax-derived peptide: Evidence for lipidic pores. *Proc Natl Acad Sci USA* 105(45):17379–17383.
49. Zhang Z, et al. (2010) Bax forms an oligomer via separate, yet interdependent, surfaces. *J Biol Chem* 285(23):17614–17627.
50. Brustovetsky T, et al. (2010) BAX insertion, oligomerization, and outer membrane permeabilization in brain mitochondria: Role of permeability transition and SH-redox regulation. *Biochim Biophys Acta* 1797(11):1795–1806.
51. Zhang Z, et al. (2016) BH3-in-groove dimerization initiates and helix 9 dimerization expands Bax pore assembly in membranes. *EMBO J* 35(2):208–236.
52. Lauterwasser J, et al. (2016) The porin VDAC2 is the mitochondrial platform for Bax retrotranslocation. *Sci Rep* 6:32994.
53. Czabotar PE, et al. (2013) Bax crystal structures reveal how BH3 domains activate Bax and nucleate its oligomerization to induce apoptosis. *Cell* 152(3):519–531.
54. Dlugosz PJ, et al. (2006) Bcl-2 changes conformation to inhibit Bax oligomerization. *EMBO J* 25(11):2287–2296.
55. Li R, et al. (2004) Dimerization of the transmembrane domain of Integrin alphaIIb subunit in cell membranes. *J Biol Chem* 279(25):26666–26673.
56. Kerppola TK (2008) Bimolecular fluorescence complementation: Visualization of molecular interactions in living cells. *Methods Cell Biol* 85:431–470.
57. Kodama Y, Hu CD (2010) An improved bimolecular fluorescence complementation assay with a high signal-to-noise ratio. *Biotechniques* 49(5):793–805.
58. Kodama Y, Hu CD (2013) Bimolecular fluorescence complementation (BiFC) analysis of protein-protein interaction: How to calculate signal-to-noise ratio. *Methods Cell Biol* 113:107–121.

Supporting Information

Supporting Information Corrected February 13, 2017

Andreu-Fernández et al. 10.1073/pnas.1612322114

SI Methods

Design and Cloning of ToxRed Bcl-2 TMD Constructs. The ToxRed plasmids were provided by William DeGrado, School of Pharmacy, University of California, San Francisco. ToxRed chimeric constructs were generated by specific primer annealing of Bcl-2 protein TMDs in the HindIII/XhoI restriction sites of ToxRed vectors (Table S1). All transmembrane sequences were codon-optimized for *E. coli* expression. TMD mutants were created by using standard site-directed mutagenesis with a commercially available Stratagene Quikchange II kit (Agilent). All molecular biology techniques were performed according to standard procedures. The maltose complementation assay was performed as described (39, 55).

ToxRed Oligomerization Assays. ToxR–Bcl-2 TMD constructs were transformed into the *malE* mutant *E. coli* MM39 strain and plated in maltose minimal-agar medium. Cells were grown in selective LB to OD_{600} 0.2 and incubated with shaking at 37 °C in maltose-minimal medium until OD_{600} 0.8. For RFP measurements, 24-well plates were adjusted to equivalent growth (OD_{600} 0.6–0.8) and the RFP emission spectra collected by a Wallac 1420 Workstation (λ_{exc} 560 and λ_{em} 595 nm). The ToxRed dominant-negative experiments to study heterooligomer formation were performed as described (31).

Western Blotting for ToxRed-TMD Constructs. Whole-cell extracts were subjected to SDS/PAGE, transferred to nitrocellulose membranes, and blotted following standard procedures. MBP primary antibody (no. E8038S) was purchased from New England Biolabs.

TOXRED Fluorometry Studies. Saturated cultures (5 mL) were centrifuged at 1,500 × *g* for 10 min and pellets resuspended in 500 μL of freshly prepared FasterBreak Cell Lysis Reagent 1× (Promega). After 15 min of mixing, lysates were centrifuged at 1,500 × *g* and fluorescence measured (λ_{exc} 584 and λ_{em} 595–610 nm) in a spectrofluorometer.

BiFC Fluorometry Studies. A total of 8×10^5 cotransfected cells (VN and VC vectors) were scraped on ice, collected in PBS, and centrifuged at 2,500 rpm for 5 min at 4 °C. Cell pellets were resuspended in 500 μL of lysis buffer (50 mM Tris HCl, pH 7.4, 150 mM NaCl, 1 mM EDTA, 1 mM EGTA, 5 mM $MgCl_2$, and 0.5% Triton X-100 containing 0.1 mM PMSF, 20 μM leupeptin, and 1 μM pepstatin) and mixed for 30 min on a rotary platform at 4 °C. Cell lysates were centrifuged at 10,000 rpm for 5 min at 4 °C, and fluorescence emission spectra were recorded (λ_{exc} 515 and λ_{em} 520–650 nm).

Cell Culture. Human colorectal carcinoma HCT116 cells, provided by Richard Youle, Porter Neuroscience Research Center, Bethesda, and Bert Vogelstein, Johns Hopkins University School of Medicine, Baltimore, were grown in McCoy's 5A medium supplemented with 10% FBS. Cultures were maintained at 37 °C in a 5% CO_2 atmosphere.

BiFC-TMD Assays. BiFC assays were performed as described (56). An improved BiFC assay with a high signal-to-noise ratio was selected to avoid background interference (57, 58). The system was adapted to clone Bax, Bcl-x_L, and Bcl-2 TMDs at the C terminus of venus protein fragments according to their natural topology in full-length proteins. In the case of Bax, some oligomerization experiments were performed in both orientations due to the high levels of cell death induction observed when the C-terminal orientation was used that interfere with proper analysis in some experimental conditions. BiFC plasmids from Addgene (catalog nos. 27097 and 22011) were modified to insert a linker (GGGGSGGGGSSGR for VN and RPACKIPNDLKQKVM-NHDKQKSGR for VC) and a NotI restriction site behind the venus fragment to clone the Bcl-2 protein TMDs in the adequate topology. Venus VN-terminal (1–154, I152L) and VC-terminal (155–238, A206K) fragments were fused with the TMD region of the different Bcl-2 proteins (Table 1). The human Bcl-2 TMD sequences were introduced by oligonucleotide annealing (Table S1). BiFC–Bcl-2 protein TMD mutant constructs were obtained by using standard site-directed mutagenesis with the Stratagene Quikchange II kit. VN and VC constructs have c–myc and HA tags, respectively, for appropriate detection.

HCT116 cells at 60–70% confluence in 96-well black plates were cotransfected with 0.05–0.1 μg of DNA constructs by using Lipofectamine 2000 or Turbofect, according to the manufacturer's instructions. Transfected cells were incubated at 37 °C for 18 h to avoid toxicity, and then venus fluorescence emission was measured by using a Wallac 1420 Workstation (λ_{exc} 510 and λ_{em} 535 nm). Transfection efficiency was monitored using a GFP-Bcl-2 TMD construct and maintained >70% in all experiments. For Western blotting analysis, cells were seeded in six-well plates, transfected with 0.5–1 μg of DNA constructs by using Turbofect, and incubated for 18 h. Total protein extracts were analyzed for chimera expression by using primary antibodies against HA C29F4 (catalog no. 3724S) and c-myc 9B11 (catalog no. 2276S) (Cell Signaling).

Smac Release from Isolated Mitochondria. Mitochondria from HCT116 cells were purified as described (13). To study Smac release in isolated mitochondria in vitro, mitochondrial outer membrane permeabilization was induced with recombinant tBid (R&D Systems; 10 nM). Mitochondria (50 μg) were incubated with TMD peptides at the indicated concentrations in 200 μL of KCl buffer [125 mM KCl, 4 mM $MgCl_2$, 5 mM Na_2HPO_4, 5 mM succinate, 0.5 mM EGTA, 15 mM Hepes–KOH (pH 7.4), and 5 μM rotenone] for 15 min at 30 °C. The mitochondria were then centrifuged for 5 min at 13,000 × *g* at 4 °C. Mitochondrial pellets corresponding to 5 μg of protein and the corresponding volume of supernatant fractions were resolved by SDS/PAGE and transferred to a nitrocellulose membrane. Smac (antibody) was monitored in the supernatant and pellet by Western blot to monitor release. Bax (antibody) and VDAC (antibody) served as loading controls.

BirA Interaction Partner Identification. HCT116 Bax/Bak DKO cells were transfected with pcDNA3-mycBioID-Bax plasmid, resulting in the expression of myc-tagged Bax/BirA fusion. After cell harvest in ice-cold PBS, the cell pellet was resuspended in SEM buffer [10 mM Hepes, pH 7.2, 250 mM sucrose, containing complete proteinase inhibitor mix (Roche), and 0.2% Triton X-100] and lysed. The cell lysate was cleared via centrifugation at 120,000 × *g* at 4 °C for 30 min, applied to a concentrator column (Vivaspin 3000 MWCO; GE Healthcare), and washed (100 mM Tris·HCl, pH 8.0, 150 mM NaCl, 5 mM EDTA, 0.1% Triton X-100, and complete proteinase inhibitor mix; Roche). The input sample (2.5%) was separated, and the remaining lysate was incubated with streptavidin agarose beads (Thermo) at 4 °C overnight. After incubation, the beads were washed four times with washing buffer and finally boiled in SDS loading buffer. Input and bead samples were resolved on a 10% SDS/PAGE and analyzed by Western blot for the indicated proteins.

Immunofluorescence. HCT116 cells were seeded on coverslips (50% confluence), transfected with equal amounts of VC/VN BiFC-TMD constructs, and incubated for 24 h at 37 °C. Mitochondria were stained with 500 nM MitoTracker (Invitrogen) for 20 min at 37 °C, and cells were fixed with 4% paraformaldehyde. The coverslips were mounted on glass slides with Mowiol/DAPI (Sigma). Confocal microscopy images were obtained by using a laser-scanning microscope 510 with a 63× objective.

Apoptosis Assays. Cell extracts were prepared from cells seeded in 3.5-cm-diameter plates at a density of 4×10^5 cells per plate. The cells were transfected with 0.75 μg of VN-Bax in the presence of a mock pcDNA3.1 (0.75 μg) vector or the same vector containing Bcl-2 or Bcl-x_L sequences. Cells were harvested after 18 h, and the pellets were resuspended in 50 μL of extraction buffer (50 mM Pipes, 50 mM KCl, 5 mM EDTA, 2 mM $MgCl_2$, and 2 mM DTT, supplemented with protease inhibitor mixture from Sigma), and kept on ice for 5 min. After the pellets were frozen and thawed three times, the cell lysates were centrifuged at 14,000 rpm for 5 min, and supernatants were collected. The total protein concentration of these cell extracts was quantified by using the bicinchoninic acid method. A total of 50 μg was mixed with 200 μL of caspase assay buffer (PBS, 10% glycerol, 0.1 mM EDTA, and 2 mM DTT) containing 20 μM Ac-DEVD-afc. Caspase activity was monitored after the release of fluorescent afc at 37 °C by using a Wallac 1420 Workstation (λ_{exc} 400 and λ_{em} 508 nm).

Statistical Analysis. All of the values represent the mean ± SD of at least three independent experiments. Significance was determined by one-way ANOVA, applying the Dunnett's test using GraphPad software. $P < 0.05$ was considered significant.

Sequences of Constructs.

BaxFL/BirA

myc-BIR-**Bax TMD**

MEQKLISEEDLDKDNTVPLKLIALLANGEFHSGEQLGE-
TLGMSRAAINKHIQTLRDWGVDVFTVPGKGYSLPEPIQ-
LLNAKQILGQLDGGSVAVLPVIDSTNQYLLDRIGELKSG-
DACIAEYQQAGRGGRGRKWFSPFGANLYLSMFWRLE-
QGPAAAIGLSLVIGIVMAEVLRKLGADKVRVKWPNDL-
YLQDRKLAGILVELTGKTGDAAQIVIGAGINMAMRRVE-
ESVVNQGWITLQEAGINLDRNTLAAMLIRELRAALEL-
FEQEGLAPYLSRWEKLDNFINRPVKLIIDKEIFGISRGID-
KGQGALLLEQDGIIKPWMGGEISLRSAEKLEL**TVTIFVA-**
GVLTASLTIWKKMG–

Bax/**Bcl-x_{Ltail}**

MDGSGEQPRGGGPTSSEQIMKTGALLLQGFIQDRAGR-
MGGEAPELALDPVPQDASTKKLSCLKRIGDELDSNME-
LQRMIAAVDTDSPREVFFRVAADMFSDGNFNWGRVVA-
LFYFASKLVLKALCTKVPELIRTIMGWTLDFLRERLLGW-
IQDQGGWDGLLSYFGTPT**WFLTGMTVAGVVLLGSLFSRK**

Bcl-x_L/**Bax$_{tail}$**

MSQSNRELVVDFLSYKLSQKGYSWSQFSDVEENRTEAP-
EGTESEMETPSAINGNPSWHLADSPAVNGATGHSSSLD-
AREVIPMAAVKQALREAGDEFELRYRRAFSDLTSQLH-
ITPGTAYQSFEQVVNELFRDGVNWGRIVAFFSFGGAL-
CVESVDKEMQVLVSRIAAWMATYLNDHLEPWIQENGGW-
DTFVEL**FGTPTWQTVTIFVAGVLTASLTIWKKMG**.

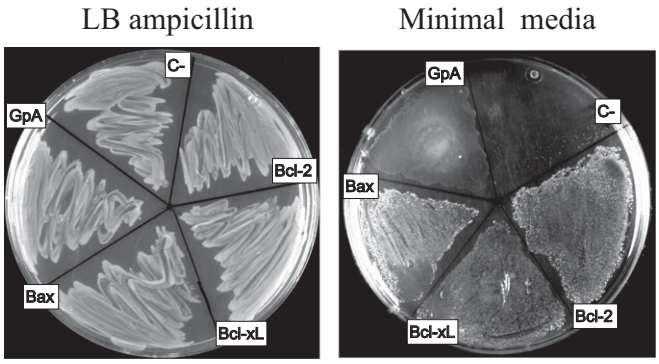

Fig. S1. Maltose complementation assay to test ToxR-TMD-MBP chimera topology. MalE-deficient *E. coli* MM39 cells were transformed with appropriate ToxR-GpA-MBP and ToxR-Bcl-MBP vectors. The MalE complementation assay indicates that chimeras containing GpA TMD and Bcl-2–related TMDs are expressed and integrated into the inner membrane of *E. coli*. The constructs were cultured on either complete medium LB (*Left*) or M9 agar containing 0.4% maltose (*Right*). Because the MM39 cell line is deficient in MBP, only cells with properly integrated ToxR chimera can survive on maltose minimal medium.

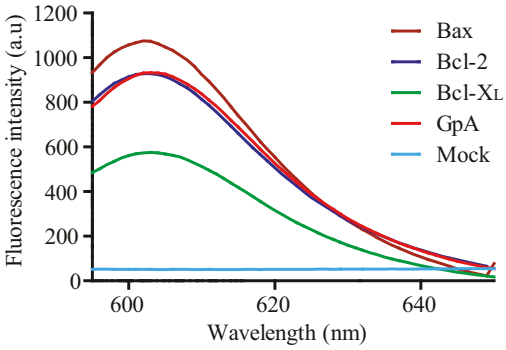

Fig. S2. Emission spectra for the ToxRed assay. For fluorescence measurements of RFP, samples from bacterial lysates were excited at 584 nm, and emission spectra were recorded from 595 to 650 nm. The mock line is for whole-cell lysates containing a control plasmid without a *ctx::mCherry* reporter.

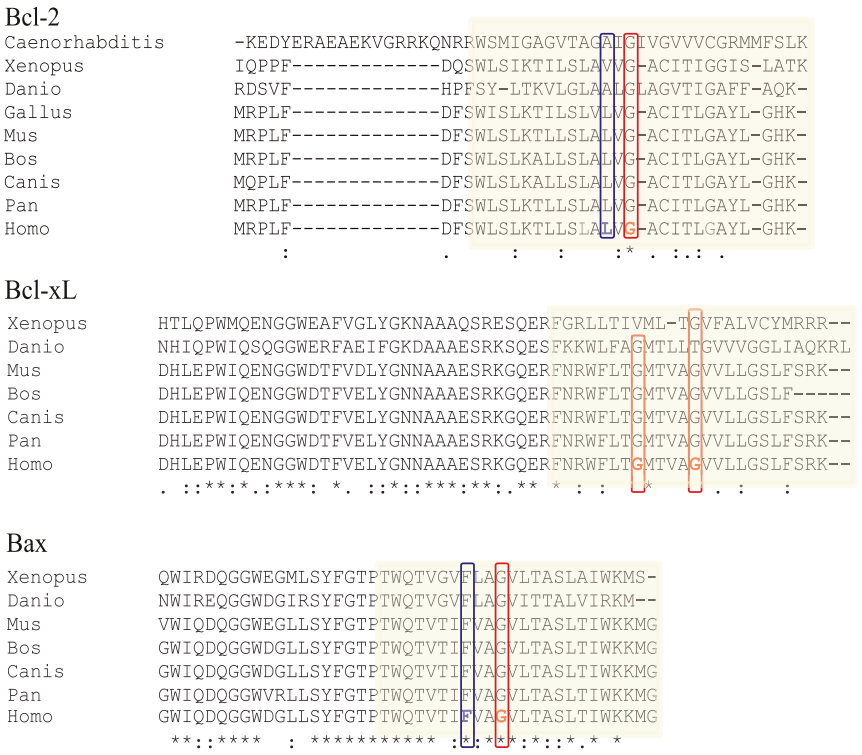

Fig. S3. Multisequence alignment of Bcl-2 TMDs from different species. Evolutionarily conserved glycine residues are boxed in red, and mutated leucine and phenylalanine residues from Bcl-2 and Bax sequences, respectively, are boxed in blue.

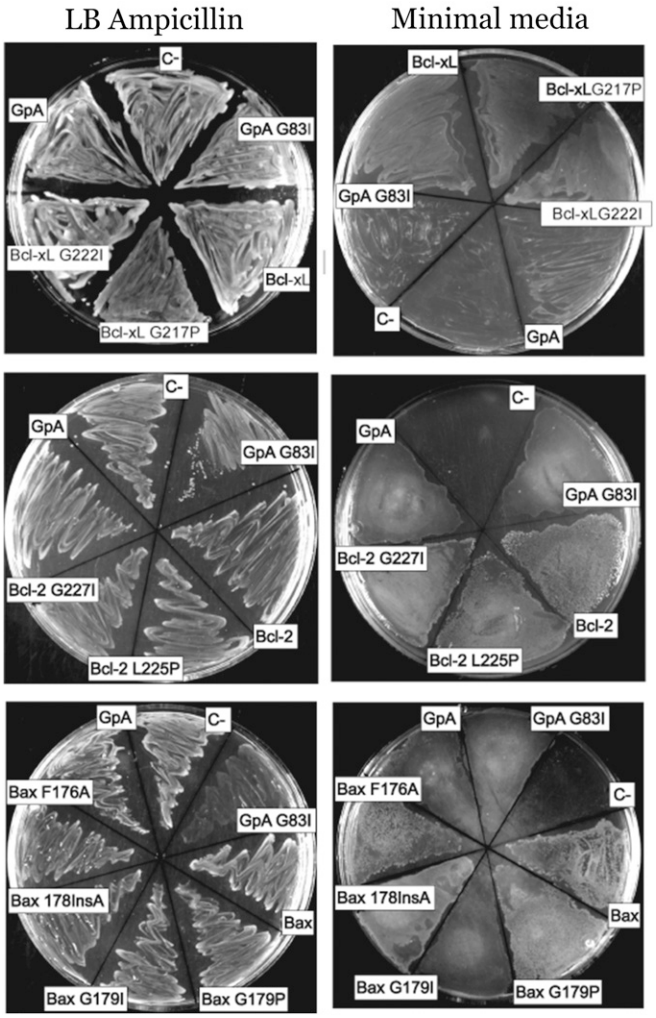

Fig. S4. Maltose complementation assay to test ToxR-TMD-MBP chimera topology in Bcl-2 mutants. MalE-deficient *E. coli* MM39 transformed with the different ToxR-TMD-MBP mutant constructs were cultured on either on complete medium LB (*Left*) or M9 agar containing 0.4% maltose (*Right*) as in Fig. S1.

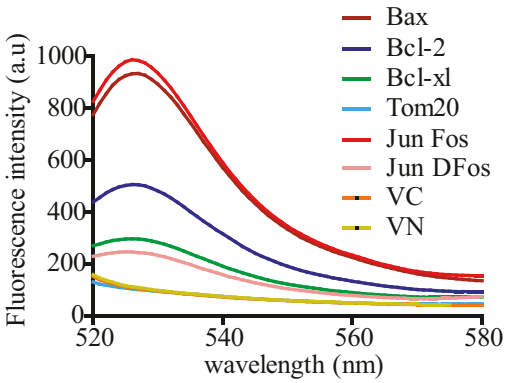

Fig. S5. Emission spectra for the BiFC assay. For fluorescence measurements, samples from cellular lysates were excited at 515 nm, and emission spectra were recorded from 520 to 580 nm. Nonoligomerizing Tom20 TMD, VN, and VC constructs were included as controls.

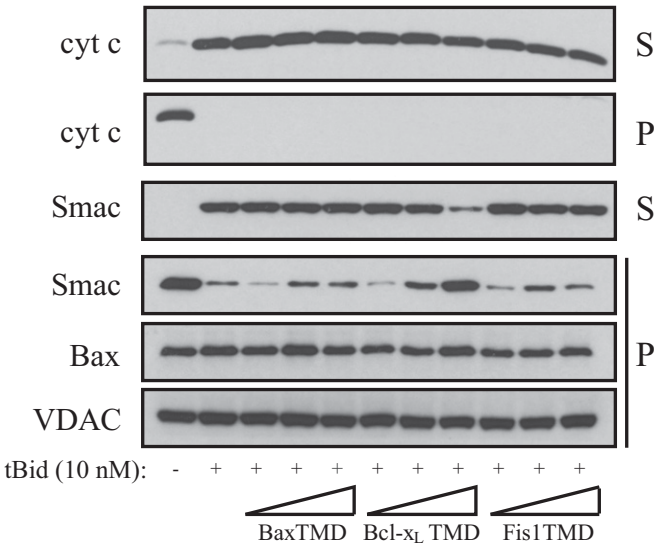

Fig. S6. Influence of Bcl-2 protein TMDs on Smac and cyt *c* release. Smac and cyt *c* release by Bax with and without tBid in the absence or presence of Bax TMD, Bcl-x_L TMD, or Fis1 TMD from purified HCT116 Bak KO mitochondria. Smac and cyt *c* were monitored in the supernatant and pellet by Western blot. VDAC served as a loading control.

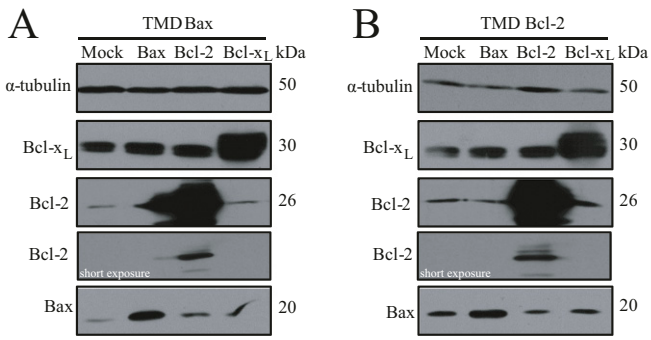

Fig. S7. Expression of FL proteins in VN/VC Bax TMD (*A*) and VN/VC Bcl-2 TMD (*B*) competition experiments using full-length Bcl-2–derived proteins from Fig. 4 in the HCT116 wild-type cell line.

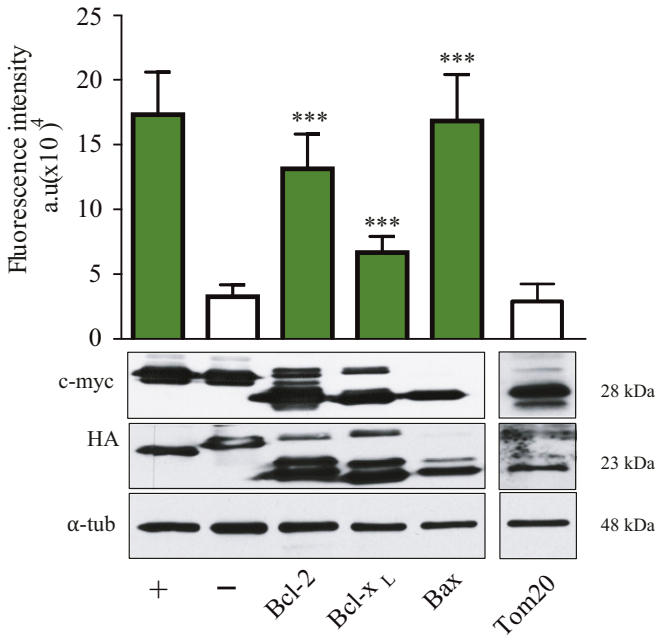

Fig. S8. Bax, Bcl-2, and Bcl-x_L homooligomerize in the OMM of HCT116 Bax/Bak DKO cells. Bax, Bcl-2, and Bcl-x_L TMD homooligomerization measured by BiFC in HCT-116 Bax/Bak DKO cells is shown. Fusion b-Fos and b-Jun proteins were used as positive controls (+), and the Δb-Fos/b-Jun pair served as negative controls (–); $n = 3$. Significant increases compared with the negative control were analyzed by using Dunnett's multiple comparison test (95% confidence interval). Chimeric protein expression is compared in *Lower* by Western blotting with the appropriate antibodies. Error bars represent the mean ± SD; $n \geq 3$. ***$P < 0.001$.

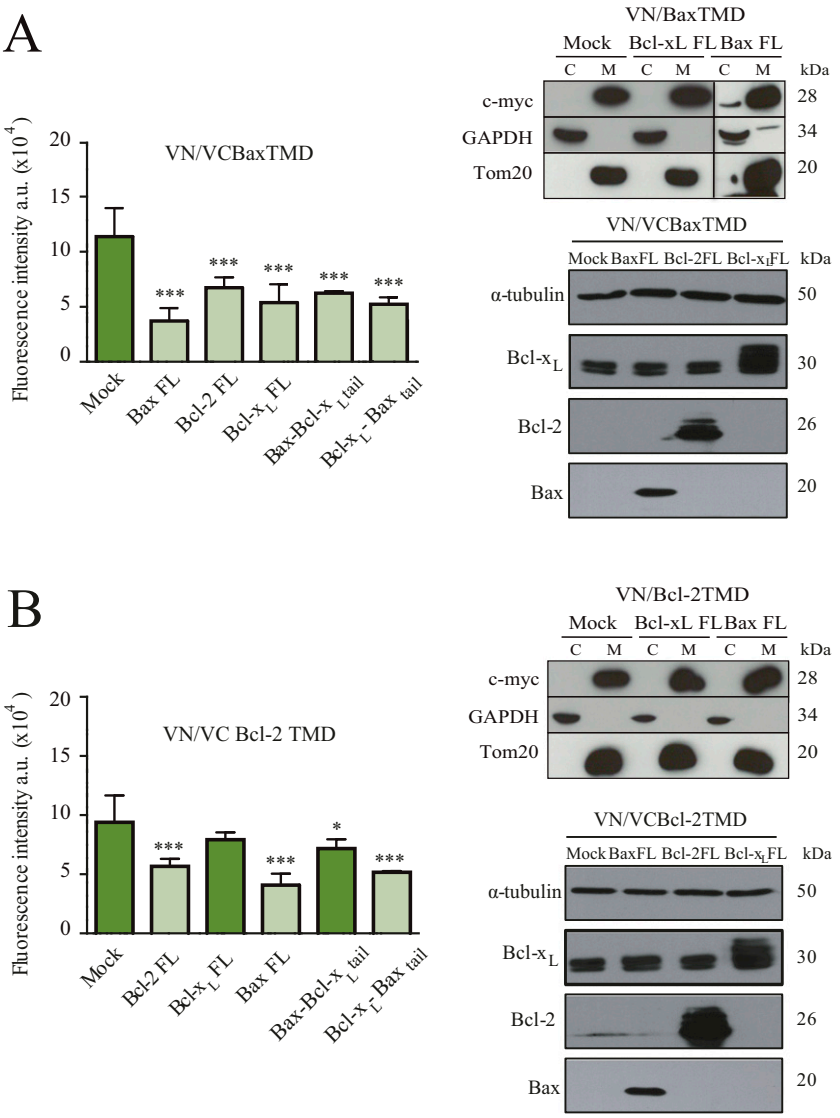

Fig. S9. Bcl-2 TMDs interact with full-length proteins in the OMM of HCT116 Bax/Bak DKO cells. (*A*) Oligomerization analysis of the Bax TMD in the presence of full-length Bax, Bcl-2, Bcl-x_L, Bax–Bcl-xL_{tail}, and Bcl-xL–Bax_{tail}. VFP reconstitution by VN/VC BaxTMD chimeras was challenged with the indicated full-length proteins in HCT116 cells (*A*, *Left*). Subcellular fractionation showed mitochondrial (M) localization of VN/Bax and VC/Bax in the absence or presence of full-length Bax and Bcl-x_L proteins (*A*, *Right Upper*). Expression of full-length proteins was analyzed by Western blot (*A*, *Right Lower*). (*B*) Oligomerization analysis of the Bcl-2 TMD in the presence of full-length Bax, Bcl-2, Bcl-x_L, Bax–Bcl-x_{Ltail}, and Bcl-x_L–Bax_{tail}. Subcellular fractionation showed mitochondrial (M) localization of VN/Bcl-2 and VC/Bcl-2 in the absence or presence of full-length Bax and Bcl-xL proteins (*B*, *Right Upper*). Expression of full-length proteins was analyzed by Western blot (*A*, *Right Lower*). $*P < 0.05$; $***P < 0.001$.

Table S1. Primers for cloning Bcl-2 protein TMDs in the ToxRed vectors

TMD	Oligo forward	Oligo reverse
Bcl-2	agctttggctgtctctgaagactctgctcagtttggccctggt-gggagcttgcatcaccctgggtgcctatctgc	tcgagcagataggcacccagggtgatgcaagctcccacca-gggccaaactgagcagagtcttcagagacagccaa
Bcl-xL	agcttttcaaccgctggttcctgacgggcatgactgtggccggc-gtggttctgctgggctcactcttcagtcggc	tcgagccgactgaagagtgagcccagcagaaccacgccgg-ccacagtcatgcccgtcaggaaccagcggttgaaa
Bax	Agcttacgtggcagaccgtgaccatctttgtggcgggagtgctc-accgcctcgctcaccatctggc	tcgagccagatggtgagcgaggcggtgagcactcccgcca-caaagatggtcacggtctgccacgaa